Screening Ionic Liquids as Candidates for Separation of Acid Gases: Solubility of Hydrogen Sulfide, Methane, and Ethane

Soheil Mortazavi-Manesh
Dept. of Chemical and Petroleum Engineering, University of Calgary, 2500 University Dr. NW, Calgary, AB T2N 1N4, Canada

Marco A. Satyro
Virtual Materials Group, Inc., 222-1829 Ranchlands Blvd. NW, Calgary, AB T3G 2A7, Canada

Robert A. Marriott
Dept. of Chemistry, University of Calgary, 2500 University Dr. NW, Calgary, AB T2N 1N4, Canada

The solubility of the major constituents of natural gas in ionic liquids (ILs) can be used to identify their potential for acid gas removal from a producing gas stream. We have developed models for the solubility of H_2S, CH_4, and C_2H_6 in ILs at typical conditions encountered in natural gas treatment. In this work, a conductor-like screening model for realistic solvation was used to predict the activity coefficients for solutes in ILs and a cubic EOS was used for vapor-phase corrections from ideality. Empirical correlations were developed to extrapolate solubilities where experimental data are not available at desired conditions; targeted in this study at 298.15 K and 2000 kPa. Over 400 possible ILs were ranked based on the higher selectivity of absorption of CO_2 and H_2S over CH_4 and C_2H_6. The best 15% (58) of promising ILs for sour gas treatment predominantly contain the anions BF_4, NO_3, and CH_3SO_4 and the cations N_{4111}, pmg, and tmg. © 2013 American Institute of Chemical Engineers AIChE J, 59: 2993–3005, 2013
Keywords: gas treatment, ionic liquids, Henry's constant, selectivity, conductor-like screening model for realistic solvation

Introduction

The production of natural gas often requires treatment processes for the separation of CO_2 and H_2S. CO_2 must be removed to meet the heating value specification for sales gas; whereas, H_2S is removed due to its toxicity and to reduce the overall release of SO_2 to the atmosphere during combustion. Acid gas ($CO_2 + H_2S$) separation processes, also known as sour gas treatment, are different from carbon capture from low pressure flue gases or enhanced oil recovery due to different temperature/pressure regimes and different fluid compositions, that is, produced sour fluids contain H_2S and, unlike flue gases, they do not contain SO_2.

Traditionally, aqueous alkanolamine solutions are used to remove CO_2 and H_2S from high-pressure hydrocarbon gas production fluids through acid-base reactions and reversible formation of soluble salt species. In addition, physical solvents such as polyglycols can be used for preferential physical dissolution of H_2S and CO_2 as in Selexol™-based plants. There is an increasing interest in exploring the advantages of replacing traditional gas sweetening solvents with ionic liquids (ILs) to determine if better conditioning processes can be designed from energy consumption in regeneration and reduced solvent loss perspectives. To conceptually explore the potential of ILs for acid gas treatment and target ILs which should be explored for commercial synthesis and production, a reliable solubility model based on experimental data is needed for initial solvent screening.

ILs are molten salts consisting of large organic cations and organic or inorganic anions, allowing them to remain liquid at or near room-temperature. There are a wide range of possible applications for ILs in the chemical industry including solvents, liquid support for chemical reactions, electrolytes, and catalysts.[1–6] Due to the ionic nature of these solvents, ILs have negligible vapor pressure which is desirable in gas treatment applications and leads to minimum waste to environment and solvent loss when regenerated in a gas treatment plant. Theoretically, no solvent loss should be expected from a traditional separation point of view, but thermal stability on regeneration as well as IL stability with respect to water and other potential components present in natural gas are important design issues that are not addressed in this work.

Experimental solubility data for pure components and applicable industrial mixtures in ILs provide a useful starting point to search for an efficient IL for gas sweetening applications. However, based on different combinations of anions and cations, there are many different ILs that can be potentially used for gas treatment. In many cases, no experimental data are available and full experimental combinatorial study would be unfeasible, especially at the pressure and

Table 1. Experimental Data Conditions for H₂S-IL Mixtures

	Purity	Data Points	T_{min} (K)	T_{max} (K)	P_{min} (kPa)	P_{max} (kPa)	Loading (max)	References
Bmim-BF₄	a	42	303.15	343.15	60.8	836	0.55	13
Bmim-PF₆	a	73	298.15	403.15	69.0	9630	7.00	13,14
Bmim-Tf₂N	>98%[c]	44	303.15	343.15	94.4	916	1.04	13
Emim-C₂SO₄	–	36	303.15	353.15	111	1100	1.00	43
Emim-PF₆	>97%	40	333.15	363.15	144.9	1933	0.56	44
Emim-Tf₂N	>99%	42	303.15	353.15	107.7	1686	1.56	44
Hmim-Tf₂N	>99%[d]	30	303.15	353.15	97.4	1050	1.14	15
Hmim-BF₄	>98%[c]	33	303.15	343.15	111	1100	1.00	15
Hmim-PF₆	>98%[c]	34	303.15	343.15	138	1090	0.79	15
HOemim-BF₄	>99.5%[e]	51	303.15	353.15	121	1066	0.33	41
HOemim-Triflate	–	42	303.15	353.15	105.9	1839	1.21	42
HOemim-PF₆	–	47	303.15	353.15	133.6	1685	0.86	42
HOemim-Tf₂N	–	41	303.15	353.15	156.2	1832	1.34	42
Omim-Tf₂N	>99.95%[d]	47	303.15	353.15	93.5	1912	2.78	45

[a]Purity >99%, water mass fraction $<10^{-4}$.
[b]Purity: 98%, water mass fraction = 0.05–0.1 mass%.[14]
[c]Water mass fraction $<10^{-2}$.
[d]Water mass fraction $<10^{-4}$.
[e]Water mass fraction <100 ppm.

temperatures experienced in gas conditioning processes. Thus, a theoretically based approach can be used to initially estimate the solubility of gases important for gas processing and reduce the number of potential solvent candidates for further study.

To develop a meaningful estimation for the solubilities of binary systems of H₂S, CO₂, CH₄, and C₂H₆, the most important components present in raw natural gas, in ILs, a model must be available to quantify the interactions between the solute molecules and the ILs' cations and anions.

Sumon and Henni[7] obtained the Henry's constant of CO₂ in ILs from a conductor-like screening model for realistic solvation (COSMO-RS)[8] predictions and assumed that the vapor phase is an ideal gas and also the solubility of CO₂ in ILs follows the Henry's law. This approach is valid at low pressure and low solubility of CO₂ in ILs. Maiti[9] has used the COSMO-RS method to calculate the chemical potential of CO₂ in ILs and used a two-parameter empirical model for calculations of the chemical potential of the pure CO₂ and used an equation of state for vapor-phase nonideality corrections. Maiti's model generates large bias and average relative error (AAR) in estimations of the solubility of CO₂ in ILs.[10,11] Mortazavi-Manesh et al.[10] modified the Maiti's model, where the bias and the AAR of the estimations were significantly reduced. Recently, Mortazavi-Manesh et. al.[11] proposed a generalized model to estimate the solubility of CO₂ in ILs in which the COSMO-RS[8] calculation was implemented to obtain the activity coefficients for CO₂ in different ILs, and a Peng–Robinson equation of state[12] was used to calculate the fugacity coefficients for high-pressure CO₂ and a semiempirical correlation was used to estimate the Henry's law constant. In this study, a similar approach is used and models are proposed to estimate the solubility of H₂S, CH₄, and C₂H₆ in ILs. No experimental data were rejected during the calibration of this model, due to limited literature solubility data for H₂S, CH₄, and C₂H₆.

Using the proposed model, the pure component solubility and the selectivity of 425 ILs solvents are compared by ranking the relative solubilities at partial pressures of 2000 kPa; whereas, a fit-for-purpose comparison could be performed for specific target fluids with different partial pressures or process specifications. Of these 425 ILs, less than 25 solubility studies have been reported in the literature for H₂S, CH₄, or C₂H₆; and only three ILs have been studied for all four gases solubilities (bmim-BF₄, bmim-PF₆, and hmim-Tf₂N).[13–27] Using the proposed models, a list of promising ILs is provided by choosing those ILs which rank in the top 28% percentile for four selectivity criteria relevant to acid gas removal (H₂S/CH₄, CO₂/CH₄, H₂S/C₂H₆, CO₂/C₂H₆), that is, those ILs which preferentially dissolve H₂S and CO₂. Some of these ILs will be further investigated through an experimental program and parallel process simulations for sour gas treatment.

Theory

In this study, the approach proposed by Mortazavi-Manesh et. al.[11] was used to develop new models describing the solubility of H₂S, CH₄, and C₂H₆. COSMO-RS was used to estimate the activity coefficients of binary mixtures of H₂S, CH₄, and C₂H₆ and different ILs. The COSMO-RS model is based on quantum chemistry calculations to predict the thermodynamic properties of a solution given its optimized electronic structure.[28–31] The procedure initially involves optimizing the atomic structure of the pure solvent molecules and solute molecules using a selected *ab initio* theory level (normally with added density functional). For COSMO-RS, the information of the resulting local polarization charge densities σ and the probability densities $P_i(\sigma)$ are used to define pseudochemical chemical potentials μ_i, using Eq. 1

$$\mu_i = \mu_i^C + \int P_i(\sigma)\mu_S(\sigma)d\sigma, \qquad (1)$$

where μ_i^C is the combinatorial contribution to the chemical potential, which accounts for the shape and size differences of the molecules in the system and μ_S is σ potential which can be interpreted as the affinity of the solvent S for the surface of polarity σ. The pseudochemical potential of compound i and is related to standard chemical potential μ_i^*, by Eq. 2[32]

$$\mu_i = \mu_i^* - RT \ln x_i. \qquad (2)$$

The activity coefficient of the solute γ_i, can be calculated using Eq. 3

Table 2. Experimental Data Conditions for CH$_4$-IL Mixtures

	Purity	Data Points	T_{min} (K)	T_{max} (K)	P_{min} (kPa)	P_{max} (kPa)	Loading (max)	References
Bmim-BF$_4$	97% mol	13	283.5	343.09	46.5	97.6	0.001	16
Bmim-CH$_3$SO$_4$	>98%wt	24	293.15	413.2	1363	8853	0.048	46
Bmim-PF$_6$	a	107	283.15	343.08	115	1399	0.011	17,18
Hmim-Tf$_2$N	>99% wt	24	293.3	413.25	886	9300	0.228	19

[a]Residual chloride of 3 ppm.[17]
[b]Minimum purity 99.9% mol, water mass fraction = 150±15 ppm.[18]

$$\gamma_i = \exp\left(\frac{\mu_i - \mu_i^o}{RT}\right), \qquad (3)$$

where μ_i° is the chemical potential of compound i in the pure compound reference state.

Previously, a model was presented for prediction of the solubility of carbon dioxide in ILs[11] in which COSMO-RS was used to predict the unsymmetrical activity coefficients for CO$_2$ in ILs, and the Peng–Robinson equation of state[12] was used to calculate the carbon dioxide fugacity coefficient and the molecular weight of ILs was used as the correlating parameter. In another study,[33] the COSMO-RS calculation was used to predict the pseudochemical potential of CO$_2$ in ILs, and the Soave–Redlich–Kwong equation of state[34] was used to calculate the fugacity coefficient of the vapor phase and a three-parameter model was proposed for standard state pseudochemical potential of CO$_2$. For this study, the COSMO-RS method[28–31] was applied using the COSMOtherm software.[35] The quantum chemical COSMO-RS calculations were performed at the density functional theory level, using the BP functional[36–38] with resolution of identity approximation and a triple-ζ valence polarized basis set.[39,40]

For equilibrium calculation, one can start with expression for fugacity equalities, Eq. 4

$$f_i^v = f_i^l. \qquad (4)$$

The subscript "i" is used to note a volatile component in the mixture; in this case, a solute such as H$_2$S, CH$_4$, or C$_2$H$_6$. In this work, any IL is assumed to have negligible vapor pressure and, therefore, does not appear in the gas phase.

The fugacity of the vapor phase, assuming that we have a pure gas is given by Eq. 5

$$f_i^v = P\phi_i. \qquad (5)$$

where ϕ_i is the fugacity coefficient for the pure component. The fugacity of the liquid phase is calculated using the unsymmetrical normalization scale and is given by Eq. 6

$$f_i^l = \gamma_i^* x_i H_i, \qquad (6)$$

where γ_i^* is the unsymmetric activity coefficient, calculated based on the symmetric activity coefficient calculated by COSMO-RS, Eq. 7

$$\gamma_i^* = \gamma_i / \gamma_i^\infty. \qquad (7)$$

The total pressure of the solute-IL system is calculated using Eq. 8

$$p = \frac{x_i \gamma_i^* H_i}{\phi_i}. \qquad (8)$$

Calculation of the total pressure is straightforward once the Henry's constant of H$_2$S, CH$_4$, or C$_2$H$_6$ in different ILs is available. Ideally, the dependency of H_i with specific ILs can be captured using a simple IL molecular parameter or property correlation. It should be noted that a ternary system (solute, anion, and cation) is considered for COSMO-RS calculations using COSMOTherm; whereas, experimental data are based on a binary system (solute and ion pair). All concentrations within this study refer to the binary system for direct comparison and/or calibration with experimental results.

The compilations of H_i have been correlated using (1) experimentally measured solubilities of H$_2$S, CH$_4$, or C$_2$H$_6$ in ILs; (2) the calculated activity coefficients; and (3) the fugacity coefficients of H$_2$S, CH$_4$, or C$_2$H$_6$ in the gas phase. The fugacity coefficients for H$_2$S, CH$_4$, or C$_2$H$_6$ were calculated using the Peng–Robinson equation of state[12]

$$\ln\phi = Z - 1 - \ln(Z - B) - \frac{A}{2\sqrt{2}B}\ln\left(\frac{Z + 2.414B}{Z - 0.414B}\right), \qquad (9)$$

where Z is the compressibility factor. The parameters A and B are defined elsewhere.[12]

Table 3. Experimental Data Conditions for C$_2$H$_6$-IL Mixtures

	Purity	Data Points	T_{min} (K)	T_{max} (K)	P_{min} (kPa)	P_{max} (kPa)	Loading (max)	References
Bmim-BF$_4$	97% mol	12	283.02	343.22	42.4	93.6	0.004	16
Bmim-PF$_6$	a	100	283.1	343.12	1	1399	0.045	17,18,20
Bmim-Tf$_2$N	>99%	63	283.1	323.1	2.1	1300	0.144	20
Hmim-Tf$_2$N	>99.5% mol[c]	90	283.3	368.4	100	13,070	0.671	21,22

[a]Residual chloride of 3 ppm.
[b]Minimum purity 99.9% mol, water mass fraction = 150±15 ppm.[18]
[c]Water mass fraction <20 ppm.[21]

Table 4. The Anions and Cations Properties (Surface Area is Calculated Using COSMOtherm Software[35])

Abbreviation	Ion name	MW (g/gmol)	Surface Area ($\times 10^{20}$ m^2)	Structure
Anions				
Tf$_2$N	Bis(trifluoromethylsulfonyl)-imide	280.147	203.48	
PF$_6$	Hexafluorophosphate	144.964	108.62	
BF$_4$	Tetrafluoroborate	86.805	90.57	
Triflate or OTF	Trifluoromethanesulfonate	149.070	127.80	
CH$_3$SO$_4$	Methylsulfate	111.098	118.64	
TFA	Trifluoroacetate	113.016	111.87	
C$_2$SO$_4$	Ethylsulfate	125.125	138.73	
EtGLEtGLeC$_2$SO$_4$	2-(2-methoxyethoxy)ethyl sulfate or Diethyleneglycolmonomethylethersulfate	199.203	221.06	
C$_8$SO$_4$	Octylsulfate	209.285	255.56	
Doc	Docusate or 1,4-bis(2-ethylhexyloxy)− 1,4-dioxobutane-2-sulfonate	421.571	466.96	
NO$_3$	Nitrate	62.005	76.40	
Cl	Chloride	35.453	52.81	Cl$^-$
DEP	Diethylphosphate	153.094	181.17	
DBP	Dibutylphosphate	209.201	260.27	
FEP	Tris(pentafluoroethyl)trifluorophosphate	445.010	260.17	

Table 4. *Continued*
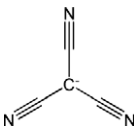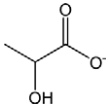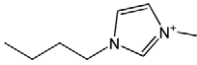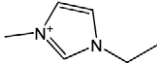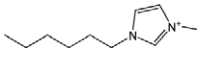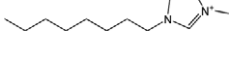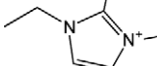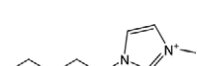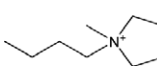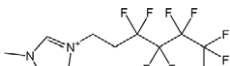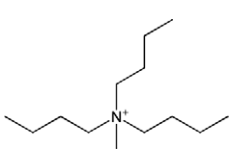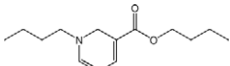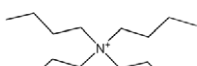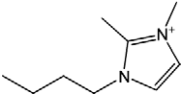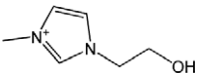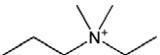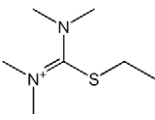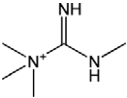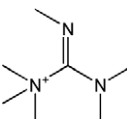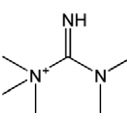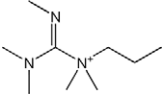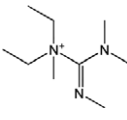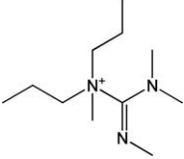
Abbreviation	Ion name	MW (g/gmol)	Surface Area ($\times 10^{20}$ m^2)	Structure
TCA	Tricyanomethanide	90.063	131.45	
L	Lactate or 2-hydroxypropanoate	89.070	116.49	
Cations				
bmim	1-butyl-3-methylimidazolium	139.2189	200.99	
emim	1-ethyl-3-methylimidazolium	111.1655	161.22	
hmim	1-hexyl-3-methylimidazolium	167.2722	241.04	
omim	1-octyl-3-methylimidazolium	195.3256	280.68	
emmim	1-ethyl-2,3-dimethylimidazolium	125.1922	175.27	
N-bupy	1-butylpyridinium	136.215	191.86	
N4111	Butyltrimethylammonium	116.2252	182.56	
pmim	1-pentyl-3-methylimidazolium	153.2456	220.99	
MeButPyrr	1-butyl-1-methylpyrrolidinium	142.2627	201.25	
C$_6$H$_4$F$_9$mim	1-methyl-3-(3,3,4,4,5,5,6,6, 6-nonafluorohexyl)imidazolium	329.1863	280.92	
hmpy	1-hexyl-3-methylpyridinium	178.295	254.11	
MeBu3N or N1444	Methyl-tributylammonium	200.3853	278.69	
b2Nic	1-butyl-nicotinic acid butyl ester	236.3313	300.58	
N4444	Tetrabutylammonium	242.4653	326.01	

Table 4. *Continued*

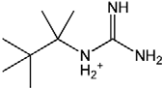| Abbreviation	Ion name	MW (g/gmol)	Surface Area ($\times 10^{20}$ m^2)	Structure
bmmim	1-butyl-2,3-dimethylimidazolium	153.2456	215.01	
HOemim	1-(2-hydroxyethane)− 3-methylimidazolium	127.165	171.44	
N2311	Ethyl-propyl-dimethylammonium	116.2252	175.36	
ETT	S-Ethyl-tetramethylisothiouronium	161.2895	207.09	
tmg	Tetramethylguanidinium	116.1853	165.15	
hmg	Hexamethylguanidinium	144.2387	196.53	
pmg	Pentamethylguanidinium	130.2120	175.67	
pmeg	Pentamethylethylguanidinium	158.2653	212.50	
pmpg	Pentamethylpropylguanidinium	172.2920	230.99	
tmdeg	Tetramethyldiethylguanidinium	172.2920	223.93	
tmdpg	Tetramethyldipropylguanidinium	200.3454	251.01	

Database Description and Model Development

Experimental solubility data for 14 H$_2$S-IL mixtures were collected and summarized in Table 1.[13–15,41–45] The purification methods, specifically drying methods, were noted. All data were equally weighted for optimization due to lack of reliable uncertainty information in the original data. This global inclusion of data is due to limited availability and is a disadvantage when compared to calibration of our previous CO$_2$ models,[10,11] where more IL solubility data were available for both calibration and external validation. The experimental H$_2$S solubility database still provides diversity of cations such as bmim, emim, hmim, HOemim, and omim. The anions in the database include ethyl sulfate and

Table 5. Recommended Parameters for H₂S-IL, CH₄-IL, and C₂H₆-IL

Component	Parameter θ	Value	AAR%	AAD (kPa)	Bias (kPa)
H_2S	Surface area	$\alpha_1 = 13.5909$, $\alpha_2 = 1.8812 \times 10^{17}$ $\beta_1 = -1243.5823$, $\beta_2 = -2.1300 \times 10^{20}$ $\varepsilon_1 = -2.3536 \times 10^{-1}$, $\varepsilon_2 = -1.1955 \times 10^{6}$	25.8	144	−32
CH_4	MW	$\alpha_1 = 13.3728$, $\alpha_2 = -5.7047 \times 10^{-3}$ $\beta_1 = 2.9415$, $\beta_2 = -8.54202 \times 10^{-2}$ $\varepsilon_1 = -5.2048 \times 10^{-14}$, $\varepsilon_2 = -2.0099 \times 10^{-18}$	25.9	115	−27
C_2H_6	Surface area	$\alpha_1 = 13.4868$, $\alpha_2 = -1.1328 \times 10^{17}$ $\beta_1 = -13.0335$, $\beta_2 = -2.7215 \times 10^{20}$ $\varepsilon_1 = -2.4451 \times 10^{-16}$, $\varepsilon_2 = -2.1930 \times 10^{3}$	21.4	67	−20

anions with fluorine as Tf₂N, PF₆, BF₄, and trifluoromethanesulfonate. Experimental data for CH₄-IL systems are summarized in Table 2. The cations included in the database are bmim and hmim, whereas the anions are BF₄, CH₃SO₄, PF₆, and Tf₂N. Experimental data for four ILs with C₂H₆, summarized in Table 3.[16–19,46] The cations included in the database are bmim and hmim, whereas the anions are BF₄, PF₆, and Tf₂N.

With the collected solubility data, activity coefficients calculated using COSMO-RS, and fugacity coefficients calculated using the Peng–Robinson equation of state,[12] several different semiempirical correlations to model the data were considered. Equation 10 was the general equation used for correlations

$$\ln H_{12} = \alpha + \frac{\beta}{T} + \frac{\varepsilon P}{T}. \qquad (10)$$

where the H_{12} is given on a mole fraction concentration scale. Due to typical conditions encountered in industrial pipelines (ca. 2000–8000 kPa for transmission) and common gas plant absorbers, we limited the data used for the development of the correlation to pressures below 8000 kPa and
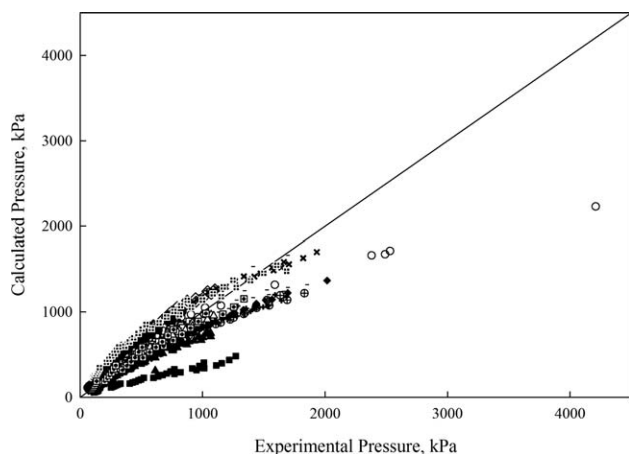
loadings below 1. Here, loading is defined as the moles of the acid gas absorbed for each mole of the solvent, thus, a maximum loading of 1 corresponds to a maximum of 0.5 in solute mole fraction.

We considered that α, β, and ε parameters of Eq. 10 are themselves functions of a physical property of IL, θ. Thus, several correlating properties were compared using a simple linear relationship

$$X = X_1 + X_2\theta \qquad (11)$$

where X can be α, β, or ε.

Using the data within the ranges described, various fitting parameters were evaluated using a nonlinear least-squares procedure described previously.[11] The most promising IL parameters discovered during this study were molecular mass (anion + cation) and total IL surface area (in m²) as calculated within the COSMOtherm software.[35] Individual ion surface areas are listed in Table 4.

The results suggest that for H₂S-IL and C₂H₆ solutes, the molecular surface area parameter results in a lower absolute AAR, absolute average deviation (AAD), and bias. For example, in the H₂S-IL case, the AAD using molecular surface area is 144 kPa compared to 155 kPa using molecular weight. For the case of C₂H₆, the AAD using a correlation with molecular surface area was 67 vs. 115 kPa for

Figure 1. Experimental total pressure of H₂S-IL mixtures vs. calculated pressure using Eqs. 8, 10, and 11 with surface area as the IL parameter.

●: bmim-BF₄,[13] ○: bmim-PF₆,[13,14] □: bmim-Tf₂N,[13] ■: emim-C₂SO₄,[43] ×: emim-PF₆,[44] ⊞: emim-Tf₂N,[44] ◇: hmim-BF₄,[15] ◆: hmim-Tf₂N,[15] Δ: hmim-PF₆,[15] ▲: HOemim-BF₄,[41] −: HOemim-Triflate,[42] +: HOemim-PF₆,[42] ⊕: HOemim-Tf₂N,[42] ⊡: omim-Tf₂N.[45]
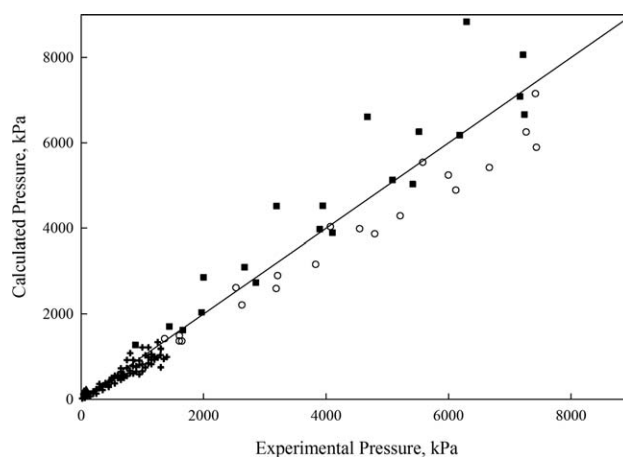

Figure 2. Experimental total pressure of CH₄-IL mixtures vs. calculated pressure using Eqs. 8, 10, and 11 with MW as the IL parameter.

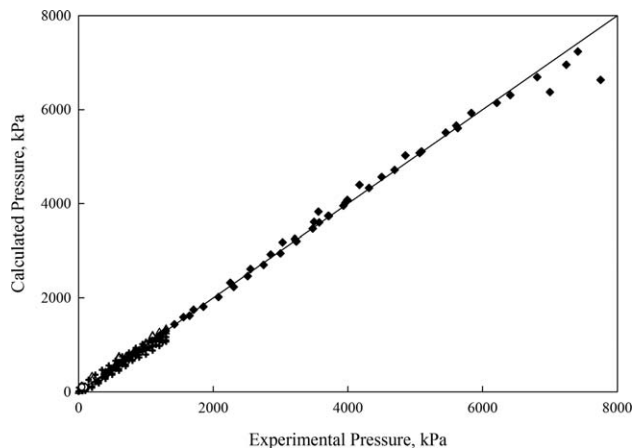▲: bmim-BF4,[16] ○: bmim-CH₃SO₄,[46] +: bmim-PF₆,[17,18] ■: hmim-Tf₂N.[19]

Figure 3. Experimental total pressure of C_2H_6-IL mixtures vs. calculated pressure using Eqs. 8, 10, and 11 with surface area as the IL parameter.

Δ: bmim-Tf$_2$N [20], ◆: hmim-Tf$_2$N [21,22], +: bmim-PF$_6$ [17,18,20], ○: bmim-BF$_4$. [16]

correlation with molecular weight. For CH_4-IL, a molecular weight correlation resulted in lower AAR, AAD, and bias (246 vs. 267 kPa for surface area). Previously, molecular weight also was found to be the better correlating factor for CO_2-ILs. [11] Although only four solute species have been tested for correlation, the results indicate that the solutes with larger dispersive interaction (larger polarizability) correlate better with the surface area of the solution molecules than those with low dispersive interaction (low van der Waal's forces). A correlation of AAD (IL molecular area)/ AAD (IL molecular weight) with molecular polarizability indicates that area is the more favorable correlation property for Henry's law with solute polarizabilities greater than 3.1 $Cm^2\ V^{-1}$.

Table 5 summarizes the recommended parameters to model the binary mixtures of H_2S, CH_4, and C_2H_6 in ILs. Results are shown as correlation plots in Figures 1–3. The results suggest that the Henry's constants for CH_4 and C_2H_6 do not have strong pressure dependence.

The Sumon and Henni's [7] method also was tested for calculating the solubility of CH_4 in ILs and found AAR of approximately 74% when compared to the experimental data cited in Table 2 against an AAR of approximately 26% obtained using the model presented here.

Despite a semiempirical Henry's law correlation, COSMO-RS calculated activity coefficients are still required to calculate solubilities at high pressures. The ILs pmg-DBP and pmpg-DEP both have the same molecular weight (325.39 g mol^{-1}); however, both CO_2 and CH_4 solubilities are slightly less for pmdg-DEP due to small differences in their respective activity coefficients (for pmg-DBP at $T = 298.15$ K and $p = 2000$ kPa, $x_{CO2} = 0.33$, and $x_{CH4} = 0.022$; and for pmpg-DEP $x_{CO2} = 0.29$ and $x_{CH4} = 0.020$). In another example, the ILs bmim-CH_3SO_4 and N-bupy-C_2SO_4 both have a molecular weight of 250.31 g mol^{-1}; for bmim-CH_3SO_4, $x_{CO2} = 0.26$ and $x_{CH4} = 0.013$ and for N-bupy-C_2SO_4, $x_{CO2} = 0.27$ and $x_{CH4} = 0.014$ (at $T = 298.15$ K and $p = 2000$ kPa).

Note that with this study it was assumed that there is no water in the system. There are studies that show the presence of water has essentially no effect on the solubility of CO_2 in ILs;[23,47,48] whereas other studies suggest that water can change the solubilities of CO_2 in ILs.[49,50] The solubility sensitivity toward water could be investigated in more detail for selected ILs.

We also note that there is potential for sulfate species to react with H_2S, for example, sulfates can react with H_2S to produce water and elemental sulfur. This may explain why the H_2S solubility data for emim-C_2SO_4 reported by Jalili et al.[43] are systematically larger than calculated values; shown in Figure 1. Jalili et al.[43] did not report any significant IL degradation; therefore, we could not justify removing the data from the calibration set.

Solubility of pure gases in ILs

Using anions and cations provided in Table 4, the solubility of CO_2[11], H_2S, CH_4, and C_2H_6 were calculate for 425 IL ion-pairs at 298.15 K and partial pressures of 2000 kPa. Partial pressures of 2000 kPa were chosen to ensure gas solubilities were being compared; whereas, H_2S at 298.15 K would be liquid above 2017 kPa. Most treatment applications for producing gas would have methane partial pressures well-above 2000 kPa. To solve the nonlinear Eq. 8 for solubilities at these conditions, either the activity coefficients would need to be recalculated using COSMO-RS at each iterative solution or a simpler activity coefficient model can be used for rapid convergence. For this comparison, the parameters of the NRTL model[51] were fitted using the activity coefficients calculated from COSMO-RS for the solubility range of gas-IL mixtures. The NRTL model was then used to solve Eq. 8 for x_i. The activity coefficients were assumed to be independent of pressure, consistent with the Henry law empirical expression, Eq. 10.

Note that the variance in anion molecular weight/area is twice the variance for the same cation properties; therefore, solubilities within these ILs are more sensitive to the anion type. ILs containing the doc, FEP, and Tf$_2$N anions show the highest average CO_2, H_2S, CH_4, and C_2H_6 solubilities; whereas, Cl, NO_3, BF$_4$, and lactate anions show the lowest average solubilities for all four of these gases, see Figures 4–7. ILs containing $C_6H_4F_9$mim, N_{4444}, and b_2Nic cations show the highest average solubility for the four solute gases. Anthony et al.[20] also found that the Tf$_2$N anion led to higher gas solubilities. A large absorption capacity for CO_2 or H_2S alone cannot be used to suggest that an IL has the potential for gas treatment/separation applications, because the solubility of CH_4 and C_2H_6 must minimized to avoid hydrocarbon losses in the solvent regeneration step. In some previous studies,[9,52] selectivity was overlooked and only the capacity of absorption was considered for screening ILs for separation of CO_2 from a gas stream.

Absorption Selectivity

For practical applications such as gas sweetening of natural gas streams containing CH_4, C_2H_6, H_2S, and CO_2, it is important to investigate relative absorption (selectivity) of the major gas stream components. Thus, we have also used the solubilities calculated for CO_2[11], H_2S, CH_4, and C_2H_6 for the 425 ILs to estimate the selectivity of absorption

Figure 4. Solubility of CO₂ in ILs at T = 298.15 K and p = 2000 kPa for different combinations of anions and cations.

Henry's constants are calculated based on molecular weight of IL.[11]

Figure 5. Solubility of H₂S in ILs at T = 298.15 K and p = 2000 kPa for different combinations of anions and cations.

Henry's constants are calculated based on surface area of ILs.

$$S_{i/j}(T,P) = \frac{x_i(T,P)}{x_j(T,P)}, \qquad (12)$$

where, S_{ij} is the selectivity of the absorbing component i over j; x_i and x_j are the mole fractions of component i and j in ILs, respectively. Note that selectivities are approximations of the actual selectivities one would experience in industrial practice because the solubilities are calculated in binary systems of solute-ILs and it is assumed that there are no tertiary solute effects. Our primary criterion for a H_2S and CO_2 separation is to choose potential solvents which will absorb more H_2S and CO_2 over CH_4 and C_2H_6. Other fit-for-purpose screening criteria can be chosen based on the application, feed gas, and outlet gas specifications.

Approximate extensions of Henry law constants for multicomponent mixtures can used to estimate ILs and water mixtures with minimum effort because good quality Henry constants for gases in water are available and semitheoretical extensions for mixture are discussed in the literature.[53] It is also worth mentioning that simple equations of state-based models can be constructed and binary interaction parameters between solute and IL solvent quickly determined, thus providing a consistent and expeditious way to extend this work to mixtures.

In some cases, processes require higher selectivity for H_2S over CO_2 or CO_2 slip. For example, (1) conventional sour gas streams with high CO_2 where sulfur recovery furnaces require high H_2S for effective performance of the Claus process, (2) some shale gas streams where CO_2 is in the percent concentration levels and H_2S is present only in the ppm concentration levels, and (3) separation of Claus tail gas streams where the desire is to recycle the remaining H_2S. Therefore, we also studied H_2S/CO_2 selectivities.

All combinations of cations and anions presented in Table 4, and S_{H_2S/CH_4}, S_{H_2S/CO_2}, S_{H_2S/C_2H_6}, S_{CO_2/CH_4}, and S_{CO_2/C_2H_6} were calculated using Eq. 12. For each $S_{i/j}$, the combinations of cations and anions were sorted in a descending order and the ILs with the highest 28th percentile were selected. Figure 4 shows the ILs which rank in the top 28% of all four selectivities desired for a basis sour gas treatment. Note that the top 28% was chosen, because this results in reducing the overall possible ILs to about 15% of the most promising ILs based on this modeling (58 ILs). Although ILs containing the doc, FEP, and Tf_2N anions were estimated to have the highest CO_2 and H_2S capacity, they were not predicted to be suitable for gas sweetening applications because they have poor S_{H_2S/CH_4} and S_{CO_2/CH_4} selectivities.

At 298.15 K and 2000 kPa, ILs containing the anions BF_4, NO_3, and CH_3SO_4 have the most number of combinations that meet the selective conditions for the top 28th percentile. ILs containing the cations N_{4111}, pmg, and tmg have the greatest number of combinations that meet the selective conditions. Table 6 shows the ILs that are within the top 28th percentile for five selectivities important for sour gas treatment (S_{H_2S/CH_4}, S_{H_2S/CO_2}, S_{H_2S/C_2H_6}, S_{CO_2/CH_4}, S_{CO_2/C_2H_6}) at 298.15 K and 2000 kPa. The advantage of this ranking and selection is that it has been used to estimate the best group of ILs to consider for further process development, thermodynamic exploration, and to justify investments on synthetic chemical routes for the production of promising ILs.

The ranking and selection of top selectivities will allow us to pursue further conceptual process designs and conduct experiments for a more focused group of ILs, 58 vs. over
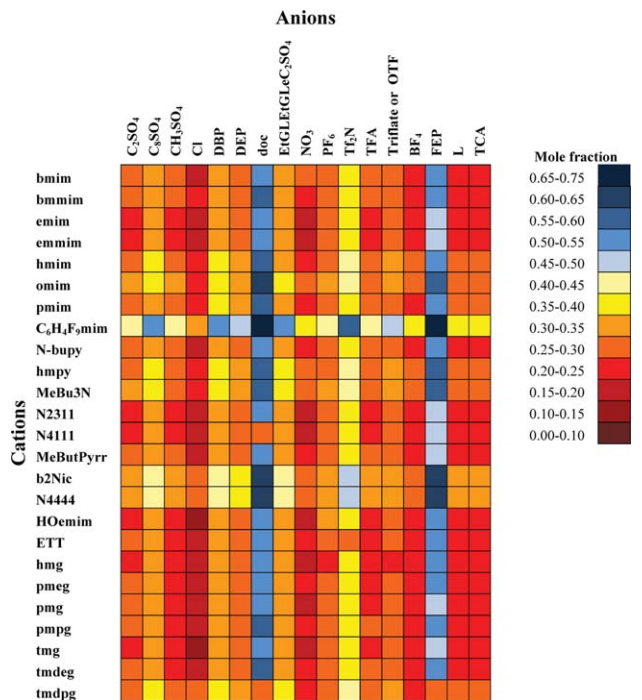
Figure 6. Solubility of CH₄ in ILs at T = 298.15 K and p = 2000 kPa for different combinations of anions and cations.

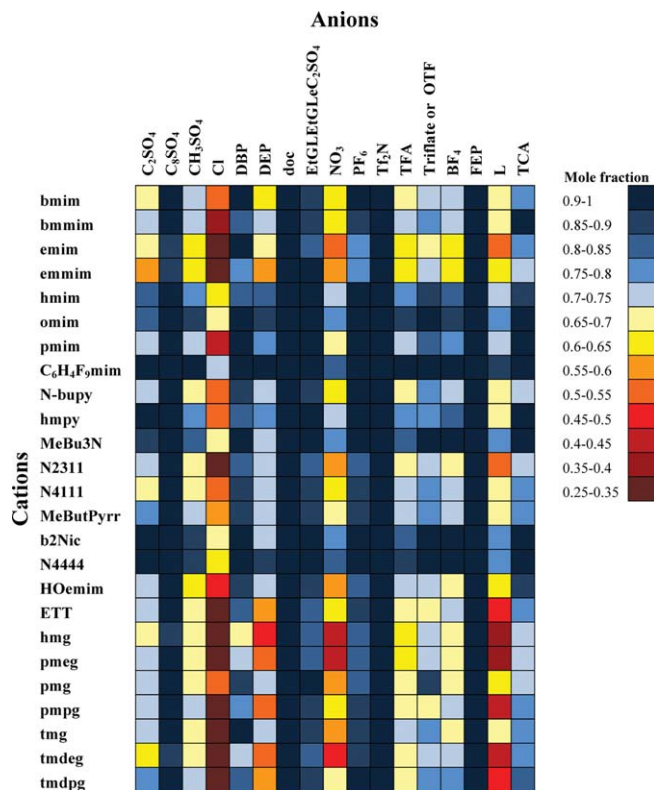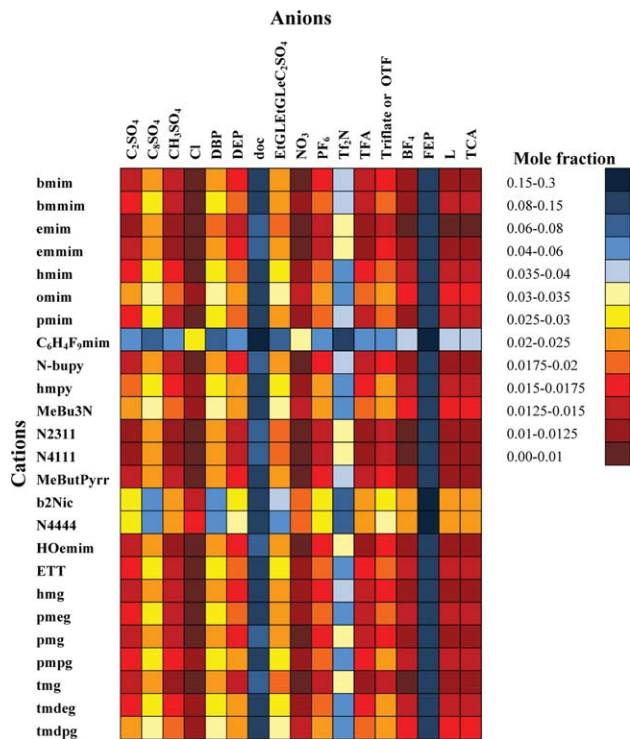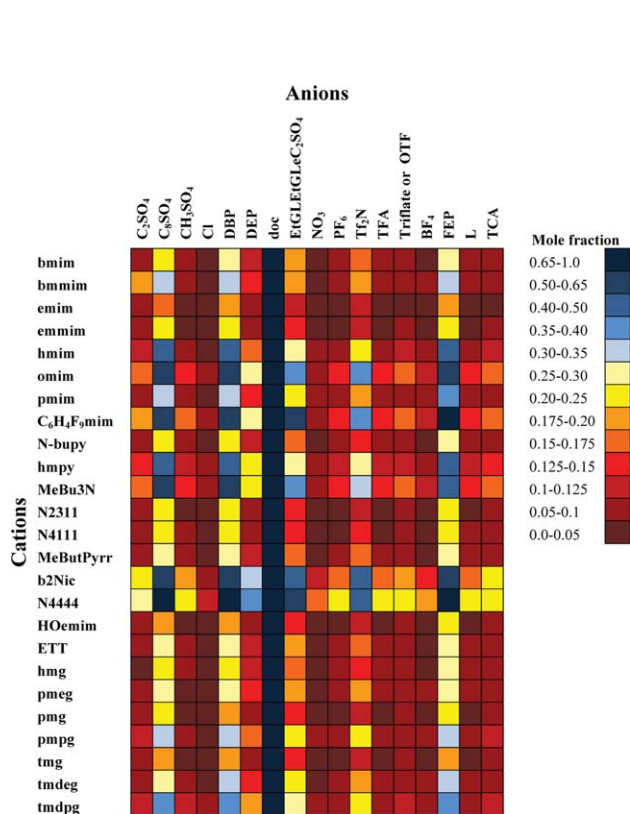Henry's constants are calculated based on the molecular weight of ILs.

Figure 7. Solubility of C₂H₆ at T = 298.15 K and 2000 kPa for different combinations of anions and cations.

Henry's constants are calculated based on surface area of ILs.

Figure 8. Investigating the selectivity of different combinations of ILs at T = 298.15 K and p = 2000 kPa.

■: ILs that are within the top 28th percentile for five selectivies important for sour gas treatment (S_{H_2S/CH_4}, S_{H_2S/CO_2}, S_{H_2S/C_2H_6}, S_{CO_2/CH_4}, and S_{CO_2/C_2H_6}).

400. Even simple properties, such as melting points are less available for this reduced set of promising ILs, that is, we were able to locate four melting points for the 58 ILs selected in Figure 8; $T_{m,\text{bmim}-CH_3SO_4} = 269$ K[54]; $T_{m,\text{bmim-Cl}} = 314$ K[55]; $T_{m,\text{emim}-NO_3} = 311$ K[56]; and $T_{m,\text{emim}-PF_6} = 331$ K.[56] Further studies are required to investigate stability, viscosity, diffusivity, effects of water in the absorption, corrosion, and other detrimental chemical reactions.

Conclusions

Semiempirical models for binary mixtures of H₂S, CH₄, and C₂H₆ dissolved in ILs were developed based on the IL molecular parameters for calculating the of Henry's constants, the use of COSMO-RS for the calculation of unsymmetrical activity coefficients, and the Peng–Robinson equation of state for the calculation of gas fugacity coefficients. This study builds on previous work for CO₂-IL binary systems and, more importantly, allows for the exploration of sour gas selectivity in ILs vs. simply pure component capacity. Here, sour gas selectivity is important in considering potential solvents for gas treatment or separation of H₂S and CO₂ from producing gas streams.

The molecular surface area of ILs were found to be the best parameter to correlation of the Henry's constants for H₂S-IL and C₂H₆-IL mixtures, and molecular weight was the best parameter for CH₄-ILs mixtures. Of the four solute gases which have been studied, Henry's constant for those
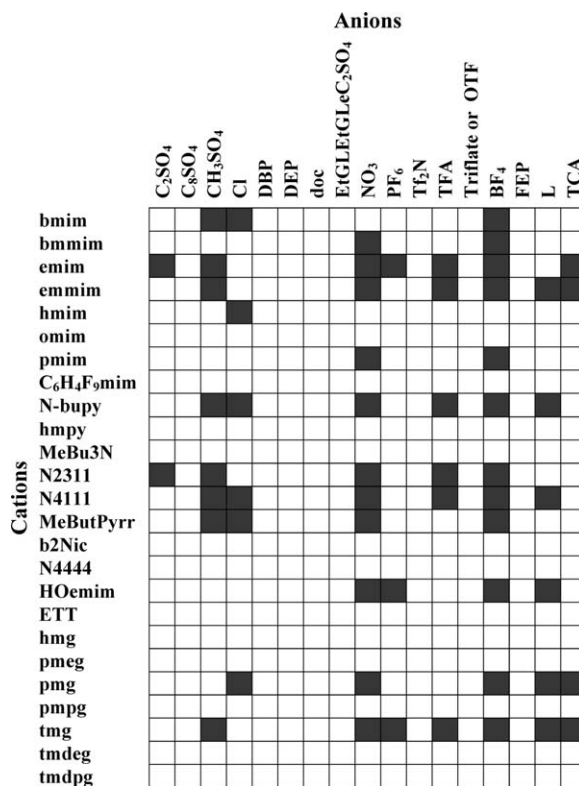
Table 6. ILs that are within the top 28th percentile for five selectivies important for sour gas treatment (S_{H_2S/CH_4}, S_{H_2S/CO_2}, S_{H_2S/C_2H_6}, S_{CO_2/CH_4}, S_{CO_2/C_2H_6}) at 298.15 K and 2000 kPa

IL	Selectivity (S)				
	$H_2S/$ CO_2	$H_2S/$ CH_4	$CO_2/$ CH_4	$H_2S/$ C_2H_6	$CO_2/$ C_2H_6
Bmim-BF$_4$	3.0	62.8	20.9	14.7	4.9
Bmim-CH$_3$SO$_4$	2.7	51.8	19.4	10.9	4.1
Bmim-Cl	2.8	66.2	23.5	17.6	6.3
Bmmim-BF$_4$	2.9	57.4	19.6	12.8	4.4
Bmmim-NO$_3$	2.7	58.4	21.4	13.3	4.9
Emim-BF$_4$	3.1	66.4	21.6	20.3	6.6
Emim-C$_2$SO$_4$	2.7	53.8	19.8	12.8	4.7
Emim-CH$_3$SO$_4$	2.8	56.1	20.1	14.5	5.2
Emim-NO$_3$	3.1	66.7	21.7	20.8	6.8
Emim-PF$_6$	2.9	55.3	19.2	18.8	6.5
Emim-TCA	3.2	74.0	23.0	14.7	4.5
Emim-TFA	2.6	53.2	20.4	14.9	5.7
Emmim-BF$_4$	3.1	61.1	19.6	17.8	5.7
Emmim-CH$_3$SO$_4$	2.7	52.3	19.7	13.4	5.0
Emmim-L	2.7	56.7	21.4	12.9	4.9
Emmim-NO$_3$	2.9	63.7	21.9	18.6	6.4
Emmim-TCA	3.0	63.6	21.5	12.1	4.1
Emmim-TFA	2.6	51.3	19.4	13.8	5.2
Hmim-Cl	2.7	61.0	22.6	12.9	4.8
HOemim-BF$_4$	3.0	62.9	21.1	19.1	6.4
HOemim-L	3.1	58.6	18.9	14.1	4.5
HOemim-NO$_3$	3.0	62.9	21.3	19.6	6.6
HOemim-PF$_6$	2.7	54.8	20.2	17.7	6.5
MeButPyrr-BF$_4$	3.1	62.3	20.3	15.0	4.9
MeButPyrr-CH$_3$SO$_4$	2.7	51.6	18.9	11.2	4.1
MeButPyrr-Cl	3.0	70.2	23.6	19.2	6.5
MeButPyrr-NO$_3$	2.9	65.5	22.3	16.2	5.5
N$_{2311}$-BF$_4$	3.1	67.8	22.0	18.7	6.1
N$_{2311}$-C$_2$SO$_4$	2.8	54.9	19.8	11.7	4.2
N$_{2311}$-CH$_3$SO$_4$	2.8	57.3	20.5	13.9	5.0
N$_{2311}$-NO$_3$	3.0	69.4	22.8	19.3	6.3
N$_{2311}$-TFA	2.8	55.9	20.0	14.4	5.1
N$_{4111}$-BF$_4$	3.2	71.9	22.4	17.9	5.6
N$_{4111}$-CH$_3$SO$_4$	2.9	59.6	20.6	13.3	4.6
N$_{4111}$-Cl	3.2	75.5	23.8	21.7	6.8
N$_{4111}$-L	2.9	64.7	22.1	12.9	4.4
N$_{4111}$-NO$_3$	3.2	72.3	22.8	18.7	5.9
N$_{4111}$-TFA	2.9	59.0	20.3	13.8	4.8
N-bupy-BF$_4$	3.1	65.2	21.3	16.5	5.4
N-bupy-CH$_3$SO$_4$	2.7	53.0	19.5	12.1	4.4
N-bupy-Cl	2.9	66.1	23.0	19.2	6.7
N-bupy-L	2.8	57.9	21.0	11.8	4.3
N-bupy-NO$_3$	2.9	63.1	22.0	16.4	5.7
N-bupy-TFA	2.7	51.3	19.4	12.3	4.6
Pmg-BF$_4$	3.1	61.6	20.0	18.7	6.1
Pmg-Cl	3.4	69.2	20.2	23.4	6.9
Pmg-L	2.9	58.6	20.6	13.8	4.8
Pmg-NO$_3$	3.1	62.8	20.2	19.4	6.3
Pmg-TCA	3.0	65.2	21.5	12.5	4.1
PMIM-BF$_4$	3.0	60.0	20.0	12.5	4.2
PMIM-NO$_3$	2.8	61.6	21.8	12.8	4.5
Tmg-BF$_4$	3.2	69.5	21.9	21.1	6.6
Tmg-CH$_3$SO$_4$	2.7	57.4	21.4	15.5	5.8
Tmg-L	3.3	65.2	20.0	15.6	4.8
Tmg-NO$_3$	3.1	68.1	22.2	21.3	6.9
Tmg-PF$_6$	3.1	62.0	19.8	20.1	6.4
Tmg-TCA	3.3	72.6	22.3	13.8	4.2
Tmg-TFA	3.1	60.2	19.3	16.6	5.3

solutes with a larger molecular polarizability (stronger van der Waal forces) correlates better with calculated IL molecular surface area vs. molecular weight. The models suggest that ILs with higher molecular surface area have higher capacity toward absorbing H$_2$S and C$_2$H$_6$, but ILs with higher molecular weight also capable of dissolving more CH$_4$.

The selectivities of absorption of acid gases (CO$_2$ and H$_2$S) over hydrocarbon (CH$_4$ and C$_2$H$_6$) in ILs at $T = 298.15$ K and $p = 2000$ kPa also were calculated for 425 IL combinations. $p = 2000$ kPa was chosen based on the high partial pressure expected in many industrial sour gas fluids; however, a similar fit-for-purpose screening can be performed for other streams. By selecting the top about 28% of IL selectivities for S_{CO_2/CH_4}, S_{H_2S/CO_2}, S_{H_2S/C_2H_6}, S_{CO_2/CH_4}, S_{CO_2/C_2H_6}, we have identified 58 of the most promising candidates for sour gas treatment, based on these models. ILs containing the anions BF$_4$, NO$_3$, and CH$_3$SO$_4$ and containing the cations N$_{4111}$, pmg, and tmg showed the most number of promising combinations. We note that to choose an IL for gas processing other physical properties and chemical stabilities for these ILs must be considered, such as melting point, viscosity, corrosivity, decomposition temperature, diffusion constant of gases into ILs, and so forth. This predictive approach can be used as an initial estimate, whereas further process exploration and experimental testing will be used to reduce the number of candidates further.

Notation

A = parameter of Eq. 9
A_{ij} = parameters of Eq. 14
AAR = absolute average relative error
AAD = absolute average deviation
B = parameter of Eq. 9
B_{ij} = parameters of Eq. 14
f_i = fugacity of component i
G_{ij} = parameters of Eq. 12
G^E = Gibbs free energy, J/mol
H = Henry's constant, kPa
IL = ionic liquids
P = pressure, kPa
$P_i(\sigma)$ = probability charge density function
COSMO-RS = conductor-like screening model for realistic solvation
R = universal gas constant, J/mol K
T = temperature, K
x_i = mole fraction of component i
X = parameter of Eq. 11
y_i = mole fraction of component i in vapor phase
y_{i-AG} = mole fraction of component i in the effluent acid gas
Z = compressibility factor

Greek letters

α = parameter of Eq. 10
β = parameter of Eq. 10
ε = parameter of Eq. 10
ϕ = fugacity coefficient
γ_i = activity coefficient of component i
γ_i^* = unsymmetrical activity coefficient of component i
γ_i^∞ = infinite dilution activity coefficient of component i in IL
η = parameter of Eq. 12
μ_i^0 = the chemical potential of compound i in the reference state of the pure compound, J/mol
μ_i^* = standard chemical potential, J/mol
μ_i = the pseudochemical potential of compound i, J/mol
μ_i^C = combinatorial contribution to the chemical potation
$\mu_s(\sigma)$ = σ-potential
v^∞ = infinite dilution volume

σ = charge density
$P_i(\sigma)$ = histogram of charge density
τ_{ij} = parameters of Eq. 12

Literature Cited

1. Wasserscheid P, Welton T, editors. Ionic liquids in synthesis, 2nd ed. Weinheim: Wiley-VCH, 2008.
2. Maase M. Erstes technisches Verfahren mit ionischen Flüssigkeiten. *Chem Unserer Zeit.* 2004;38(6):434–435.
3. Freemantle M. BASF'S smart ionic liquid. *Chem Eng News.* 2003;81(13):9.
4. Rogers RD, Seddon KR. Ionic liquids: solvents of the future? *Science.* 2003;302(5646):792–793.
5. Seddon KR. Ionic liquids: a taste of the future. *Nat Mater.* 2003;2(6):363–365.
6. Abbott AP, Capper G, Davies DL, Rasheed RK. Ionic liquid analogues formed from hydrated metal salts. *Chem Eur J.* 2004;10(15):3769–3774.
7. Sumon KZ, Henni A. Ionic liquids for CO2 capture using COS-MO-RS: effect of structure, properties and molecular interactions on solubility and selectivity. *Fluid Phase Equilib.* 2011;310(1–2):39–55.
8. Klamt A, Schuurmann G. COSMO: a new approach to dielectric screening in solvents with explicit expressions for the screening energy and its gradient. *J Chem Soc Perkin Trans 2.* 1993;(5):799–805.
9. Maiti A. Theoretical screening of ionic liquid solvents for carbon capture. *ChemSusChem.* 2009;2(7):628–631.
10. Mortazavi-Manesh S, Satyro M, Marriott RA. Modeling carbon dioxide solubility in ionic liquids. *Can J Chem Eng.* 2012;9999:1–7.
11. Mortazavi-Manesh S, Satyro M, Marriott RA. A semiempirical Henry's law expression for carbon dioxide dissolution in ionic liquids. *Fluid Phase Equilib.* 2011;307(2):208–215.
12. Peng D-Y, Robinson DB. A new two-constant equation of state. *Ind Eng Chem Fund.* 1976;15(1):59–64.
13. Jalili AH, Rahmati-Rostami M, Ghotbi C, Hosseini-Jenab M, Ahmadi AN. Solubility of H2S in ionic liquids [bmim][PF6], [bmim][BF4], and [bmim][Tf2N]. *J Chem Eng Data.* 2009;54(6):1844–1849.
14. Jou F-Y, Mather AE. Solubility of hydrogen sulfide in [bmim][PF6]. *Int J Thermophys.* 2007;28(2):490–495.
15. Rahmati-Rostami M, Ghotbi C, Hosseini-Jenab M, Ahmadi AN, Jalili AH. Solubility of H2S in ionic liquids [hmim][PF6], [hmim][BF4], and [hmim][Tf2N]. *J Chem Thermodyn.* 2009;41(9):1052–1055.
16. Jacquemin J, Costa Gomes MF, Husson P, Majer V. Solubility of carbon dioxide, ethane, methane, oxygen, nitrogen, hydrogen, argon, and carbon monoxide in 1-butyl-3-methylimidazolium tetrafluoroborate between temperatures 283 K and 343 K and at pressures close to atmospheric. *J Chem Thermodyn.* 2006;38(4):490–502.
17. Anthony JL, Maginn EJ, Brennecke JF. Solubilities and thermodynamic properties of gases in the ionic liquid 1-n-butyl-3-methylimidazolium hexafluorophosphate. *J Phys Chem B.* 2002;106(29):7315–7320.
18. Jacquemin J, Husson P, Majer V, Gomes MFC. Low-pressure solubilities and thermodynamics of solvation of eight gases in 1-butyl-3-methylimidazolium hexafluorophosphate. *Fluid Phase Equilib.* 2006;240(1):87–95.
19. Kumełan J, Pérez-Salado Kamps Á, Tuma D, Maurer G. Solubility of the single gases methane and xenon in the ionic liquid [hmim][Tf2N]. *Ind Eng Chem Res.* 2007;46(24):8236–8240.
20. Anthony JL, Anderson JL, Maginn EJ, Brennecke JF. Anion effects on gas solubility in ionic liquids. *J Phys Chem B.* 2005;109(13):6366–6374.
21. Costa Gomes MF. Low-pressure solubility and thermodynamics of solvation of carbon dioxide, ethane, and hydrogen in 1-hexyl-3-methylimidazolium bis(trifluoromethylsulfonyl)amide between temperatures of 283 K and 343 K. *J Chem Eng Data.* 2007;52(2):472–475.
22. Florusse LJ, Raeissi S, Peters CJ. High-pressure phase behavior of ethane with 1-hexyl-3-methylimidazolium bis(trifluoromethylsulfonyl)imide. *J Chem Eng Data.* 2008;53(6):1283–1285.
23. Aki SNVK, Mellein BR, Saurer EM, Brennecke JF. High-pressure phase behavior of carbon dioxide with imidazolium-based ionic liquids. *J Phys Chem B.* 2004;108(52):20355–20365.
24. Cadena C, Anthony JL, Shah JK, Morrow TI, Brennecke JF, Maginn EJ. Why is CO2 so soluble in imidazolium-based ionic liquids? *J Am Chem Soc.* 2004;126(16):5300–5308.
25. Shiflett MB, Yokozeki A. Solubilities and diffusivities of carbon dioxide in ionic liquids: [bmim][PF6] and [bmim][BF4]. *Ind Eng Chem Res.* 2005;44(12):4453–4464.
26. Shiflett MB, Yokozeki A. Solubility and diffusivity of hydrofluorocarbons in room-temperature ionic liquids. *AIChE J.* 2006;52(3):1205–1219.
27. Shiflett MB, Yokozeki A. Solubility of CO2 in room-temperature ionic liquid [hmim][Tf2N]. *J Phys Chem B.* 2007;111(8):2070–2074.
28. Klamt A. Conductor-like screening model for real solvents: a new approach to the quantitative calculation of solvation phenomena. *J Phys Chem.* 1995;99(7):2224–2235.
29. Klamt A, Jonas V, Burger T, Lohrenz JCW. Refinement and parametrization of COSMO-RS. *J Phys Chem A.* 1998;102(26):5074–5085.
30. Klamt A. COSMO-RS: From Quantum Chemistry to Fluid Phase Thermodynamics and Drug Design, 1st ed. Amsterdam: Elsevier, 2005.
31. Eckert F, Klamt A. Fast solvent screening via quantum chemistry: COSMO-RS approach. *AIChE J.* 2002;48(2):369–385.
32. Naim AB. Solvation Thermodynamics. New York: Plenum Press, 1987.
33. Mortazavi-Manesh S, Satyro M, Marriott RA. Modeling carbon dioxide solubility in ionic liquids. *Can J Chem Eng.* In press.
34. Soave G. Equilibrium constants from a modified Redlich-Kwong equation of state. *Chem Eng Sci.* 1972;27(6):1197–1203.
35. Eckert F, Klamt A, Steffen C, Schroer A, Thomas K. COSMO-thermX [computer program]. Version c21_0108. Leverkusen: COS-MOlogic GmbH & CO. KG and Ryoka Systems Inc., 2008.
36. Becke AD. Density-functional exchange-energy approximation with correct asymptotic behavior. *Physical Rev A.* 1988;38:3098–3100.
37. Vosko SH, Wilk L, Nusair M. Accurate spin-dependent electron liquid correlation energies for local spin density calculations: a critical analysis. *Can J Phys.* 1980;58:1200–1211.
38. Perdew JP. Density-functional approximation for the correlation energy of the inhomogeneous electron gas. *Phys Rev B.* 1986;33:8822–8824.
39. Schafer A, Huber C, Ahlrichs R. Fully optimized contracted Gaussian basis sets of triple zeta valence quality for atoms Li to Kr. *J Chem Phys.* 1994;100:5829–5835.
40. Eichkorn K, Weigend F, Treutler O, Ahlrichs R. Auxiliary basis sets for main row atoms and transition metals and their use to approximate coulomb potentials. *Theor Chem Acc.* 1997;97:119–124.
41. Shokouhi M, Adibi M, Jalili AH, Hosseini-Jenab M, Mehdizadeh A. Solubility and diffusion of H2S and CO2 in the ionic liquid 1-(2-hydroxyethyl)−3-methylimidazolium tetrafluoroborate. *J Chem Eng Data.* 2009;55(4):1663–1668.
42. Sakhaeinia H, Taghikhani V, Jalili AH, Mehdizadeh A, Safekordi AA. Solubility of H2S in 1-(2-hydroxyethyl)−3-methylimidazolium ionic liquids with different anions. *Fluid Phase Equilib.* 2010;298(2):303–309.
43. Jalili AH, Mehdizadeh A, Shokouhi M, Ahmadi AN, Hosseini-Jenab M, Fateminassab F. Solubility and diffusion of CO2 and H2S in the ionic liquid 1-ethyl-3-methylimidazolium ethylsulfate. *J Chem Thermodyn.* 2010;42(10):1298–1303.
44. Sakhaeinia H, Jalili AH, Taghikhani V, Safekordi AA. Solubility of H2S in ionic liquids 1-ethyl-3-methylimidazolium hexafluorophosphate ([emim][PF6]) and 1-ethyl-3-methylimidazolium bis(trifluoromethyl)sulfonylimide ([emim][Tf2N]). *J Chem Eng Data.* 2010;55(12):5839–5845.
45. Jalili AH, Safavi M, Ghotbi C, Mehdizadeh A, Hosseini-Jenab M, Taghikhani V. Solubility of CO2, H2S, and their mixture in the ionic liquid 1-Octyl-3-methylimidazolium bis(trifluoromethyl)sulfonylimide. *J Phys Chem B.* 2012;116(9):2758–2774.
46. Kumełan J, Pérez-Salado Kamps Á, Tuma D, Maurer G. Solubility of the single gases methane and xenon in the ionic liquid [bmim][CH3SO4]. *J Chem Eng Data.* 2007;52(6):2319–2324.
47. Baltus RE, Culbertson BH, Dai S, Luo H, DePaoli DW. Low-pressure solubility of carbon dioxide in room-temperature ionic liquids measured with a quartz crystal microbalance. *J Phys Chem B.* 2003;108(2):721–727.
48. Scovazzo P, Camper D, Kieft J, Poshusta J, Koval C, Noble R. Regular solution theory and CO2 gas solubility in room-temperature ionic liquids. *Ind Eng Chem Res.* 2004;43(21):6855–6860.

49. Blanchard LA, Gu Z, Brennecke JF. High-pressure phase behavior of ionic liquid/CO_2 systems. *J Phys Chem B*. 2001;105(12): 2437–2444.

50. Fu D, Sun X, Pu J, Zhao S. Effect of water content on the solubility of CO2 in the ionic liquid [bmim][PF_6]. *J Chem Eng Data*. 2006;51(2):371–375.

51. Renon H, Prausnitz JM. Local compositions in thermodynamic excess functions for liquid mixtures. *AIChE J*. 1968;14(1):135–144.

52. Zhang X, Liu Z, Wang W. Screening of ionic liquids to capture CO_2 by COSMO-RS and experiments. *AIChE J*. 2008;54(10): 2717–2728.

53. O'Connell JP, Haille JM. Thermodynamics Fundamentals for Applications. New York: Cambridge University Press: 2005.

54. Fernández A, Torrecilla JS, García J, Rodríguez F. Thermophysical properties of 1-ethyl-3-methylimidazolium ethylsulfate and 1-butyl-3-methylimidazolium methylsulfate ionic liquids. *J Chem Eng Data*. 2007;52(5):1979–1983.

55. Fredlake CP, Crosthwaite JM, Hert DG, Aki SNVK, Brennecke JF. Thermophysical properties of imidazolium-based ionic liquids. *J Chem Eng Data*. 2004;49(4):954–964.

56. Wilkes JS, Zaworotko MJ. Air and water stable 1-ethyl-3-methylimidazolium based ionic liquids. *J Chem Soc Chem Commun*. 1992:965–967.